Proceedings of Meetings on Acoustics

Volume 19, 2013 http://acousticalsociety.org/

ICA 2013 Montreal
Montreal, Canada
2 - 7 June 2013

Architectural Acoustics

Session 1pAAa: Advanced Analysis of Room Acoustics: Looking Beyond ISO 3382 II

1pAAa7. Robustness analysis of room equalization for soundfield reproduction within a region

Dumidu S. Talagala*, Wen Zhang and Thushara D. Abhayapala

***Corresponding author's address: Research School of Engineering, College of Engineering and Computer Science, Australian National University, Canberra, 0200, ACT, Australia, dumidu.talagala@anu.edu.au**

Recent works on soundfield reproduction have presented several methods of recreating a desired soundfield within a region. Estimation or prior knowledge of the inverse reverberant channels now becomes an essential element of equalizing the room effects. However, it has been shown that designing point-to-point equalizers by sampling the reverberant soundfield is only practical within a few tenths of a wavelength of the sampled locations. This work investigates the robustness of the equalization process applied to a region, with respect to changing of actual microphone positions from their expected locations. We use a modal description of the equalized soundfield to obtain theoretical results for region equalization error due to positioning errors. Simulation results suggest that equalizing the reverberant soundfield recorded at multiple positions around the edge of the reproduction region is more immune to the positioning errors.

Published by the Acoustical Society of America through the American Institute of Physics

Received 21 Jan 2013; published 2 Jun 2013

INTRODUCTION

Equalizing the effects of reverberation is an important problem in soundfield reproduction. This function is performed by a room equalizer, which acts as a set of inverse filters that equalize the effects of the room using the room impulse response measurements at a number of known locations [1]. The basic concept of the equalization filter has been successfully extended to the reproduction of a desired soundfield in a region [2, 3], where the room impulse response is measured at the edge of the reproduction region. However, calculating the desired soundfield requires knowledge of the loudspeaker and microphone positions, and any perturbations of the actual positions can result in degraded reproduction performance. In this paper, we observe the effects of these perturbations on the reproduced soundfield in a region.

A critical factor affecting the performance of a room equalizer is the degree of change in the room transfer function between the desired and perturbed microphone or loudspeaker positions. The impact on the room equalizer is minimized where the degree of change is minimal, and it is maximized where significant changes are observed. Reverberation is a result of multiple reflections off walls and other objects and creates a multipath propagation scenario, and is the primary source of variability in the channel transfer function. Studies on reverberant room acoustics [4] suggest that the room transfer function exhibits significant fluctuations between adjacent locations, where small perturbations of the microphone positions can result in a significant reproduction error. It has been noted in [5] that the room configuration does not have a significant impact on the size of the region that can be equalized, which is approximately limited to a tenth of an acoustic wavelength ($\lambda/10$) around the desired locations. Further, the equalization process is ineffective outside this small region [5, 6], which implies that a large number of microphones maybe needed to equalize a larger region. These results have called into question the robustness and practicality of room equalization when applied to large areas.

The soundfield reproduction methods in [2, 3, 7] describe a measured soundfield using spatial harmonics [8, 9] or Wave Field Synthesis [10, 11]. They model acoustic wave propagation in space and can be used to characterise any soundfield as a specific linear combination of the basis functions in 2-D or 3-D space. Hence, the measured or desired soundfield within a region can be characterised using a set of fixed coefficients that can be obtained by sampling the soundfield at the edge of the region of interest. This decouples the spatial variation of the soundfield from the actual sound source [12], and simplifies the robustness analysis of the equalization process due to spatial perturbations.

In this paper, we use cylindrical harmonics to describe the soundfield in 2-D space. We briefly describe the equalization process and show that two types of spatial perturbations exist. They are categorised into radial perturbations from the origin of the region of interest and angular perturbations around the origin. We describe the theoretically expected behaviour of each type of perturbation and use simulations examples to observe the normalized equalization error and normalized region reproduction error behaviour for plane wave and point source reproduction.

PROBLEM STATEMENT

Consider the reproduction of a desired soundfield in a region of interest within a reverberant room. Equalization of the room response is essential, and measurements of the room impulse response and the loudspeaker, microphone positions become critical parameters that affect the performance the room equalizer. In this paper, we consider the robustness of the equalization process to perturbations in the locations that the room response is measured, i.e., mispositioning of the equalizer microphones. We consider the 2-D reproduction of a line source in a reverberant room, and observe the effects of radial and angular perturbations of the microphone positions.

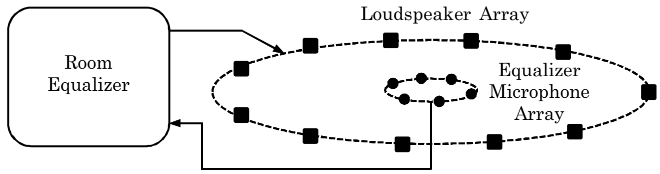

FIGURE 1: Loudspeaker and microphone array configuration.

Figure 1 above illustrates the loudspeaker and microphone configuration used for 2-D soundfield reproduction. An equalizer array of Q microphones encloses the region of interest $\mathscr{R}$ and measures the reverberant channel, while an array of P loudspeakers generate the desired soundfield. Characterisation of the soundfield and the equalization process is described below.

Soundfield Characterisation

The sound pressure measured at any point within a source free region can be expressed using the inward propagating solutions to the wave equation [12]. In 2-D space this is given by the summation

$$Y(\mathbf{x};\omega,t) = \sum_{n=-\infty}^{\infty} \beta_n(\omega,t) J_n(kx) e^{in\phi_x}, \tag{1}$$

where $J_n(\cdot)$ and $e^{(\cdot)}$ are the Bessel and exponential functions that form the orthogonal basis of 2-D space. $\mathbf{x} \equiv (x, \phi_x)$ represents the coordinates of the measurement location, $k = \omega/c$ is the wave number at a frequency ω and the speed of sound is c. The soundfield coefficients $\beta_n(\omega,t)$ describe the measured soundfield, thus, by ensuring that the measured soundfield coefficients in $\mathscr{R}$ are the same as the desired soundfield, the reverberation effects can be equalized [1–3].

Equalization of Reverberation Effects using Loudspeakers

Typically, soundfield reproduction applications perform any reverberation equalization at the loudspeakers. This requires estimation of the reverberant channel, and it has been shown that a region can be equalized by sampling the soundfield at the edge of the reproduction region [2, 3]. Given that Q satisfies the sampling requirements [2, 7] for the region $\mathscr{R}$ at a frequency ω, the loudspeaker input signals can be obtained as follows.

The measured soundfield pressure at the Q equalizer microphones can be expressed in the matrix form

$$\mathbf{Y_q}(\omega,t) = \mathbf{H_{pq}}(\omega)\mathbf{X_p}(\omega,t), \tag{2}$$

where $\mathbf{Y_q}(\omega,t) = \left[\, Y_1(\omega,t) \, \cdots \, Y_Q(\omega,t) \,\right]^T$ are the pressure measurements at the microphone array and $\mathbf{X_p}(\omega,t) = \left[\, X_1(\omega,t) \, \cdots \, X_P(\omega,t) \,\right]^T$ are the loudspeaker driving signals. $\mathbf{H_{pq}}(\omega)$ represents the channel transfer function matrix, including the reverberation effects, and can be estimated using a set of known loudspeaker input signals for $\mathbf{X_p}(\omega,t)$. Thus, if the desired soundfield pressure at the Q microphones is $\mathbf{Y^d_q}(\omega,t)$, the loudspeaker input signals become

$$\mathbf{X_p}(\omega,t) = \left[\mathbf{H_{pq}}(\omega)\right]^{\dagger} \mathbf{Y^d_q}(\omega,t), \tag{3}$$

where $\left[\mathbf{H_{pq}}(\omega)\right]^{\dagger}$ represents the Moore-Penrose pseudoinverse of the estimated channel transfer function matrix.

Since the calculation of $\mathbf{Y^d_q}(\omega,t)$ requires the knowledge of the loudspeaker and microphone positions, any mispositioning of the equalizer array will naturally degrade the performance of the room equalizer [5]. However, (3) does not describe the performance implications of perturbations in the equalizer microphone positions. The following section describes the different types of perturbations and their effect on the performance of the room equalizer.

EFFECTS OF PERTURBATION IN SOUNDFIELD REPRODUCTION

Consider a Q microphone circular array of radius r enclosing the region of interest. From (1), the desired soundfield pressure at the q^{th} microphone at $\mathbf{x_q} \equiv (r, \phi_q)$ can be expressed as

$$Y_q^d(\mathbf{x_q}; \omega, t) = \sum_{n=-N}^{N} \beta_n^d(\omega, t) J_n(kr) e^{in\phi_q}, \tag{4}$$

where $\beta_n^d(\omega, t)$ are the desired soundfield coefficients and N is a mode truncation for a specified error [2, 7]. In 2-D the desired soundfield coefficients are given by

$$\beta_n^d(\omega, t) = \begin{cases} (-i)^n e^{-in\phi_y} & : \text{Plane wave}, \\ \mathscr{H}_n^{(2)}(ky) e^{-in\phi_y} & : \text{Point source}, \end{cases} \tag{5}$$

where $\mathbf{y} \equiv (y, \phi_y)$ is the virtual source location with respect to the origin of the reproduction region and $\mathscr{H}_n^{(2)}(\cdot)$ is the n^{th} order Hankel function of the second kind [12]. Equation (4) suggests that two types of position perturbations exist; radial and angular perturbations. Next, we consider the effects of these perturbations on the soundfield reproduced by (5).

Radial Perturbations

Consider the case where a Q microphone equalizer array is located at a radial distance $r + \delta r$ from the origin of $\mathscr{R}$. From (1), the soundfield measured at the q^{th} microphone is given by

$$Y(\mathbf{x_q}; \omega, t) = \sum_{n=-N}^{N} \beta_n(\omega, t) J_n(kr + k\delta r) e^{in\phi_q}. \tag{6}$$

However, since the room equalizer attempts to reproduce the desired soundfield given in (4), the soundfield coefficients of the actual reproduced soundfield becomes

$$\beta_n(\omega, t) = \beta_n^d(\omega, t) \frac{J_n(kr)}{J_n(kr + k\delta r)}. \tag{7}$$

The perturbation factor $J_n(kr)/J_n(kr + k\delta r)$ is an unbounded function, thus, the equalization error and region reproduction error will also be unbounded and varies with r, δr, n and k.

Angular Perturbations

Now consider the scenario where the Q microphone circular array undergoes a rotation $\delta\phi$ about the origin of $\mathscr{R}$. The measured soundfield at the q^{th} microphone now becomes

$$Y(\mathbf{x_q}; \omega, t) = \sum_{n=-N}^{N} \beta_n(\omega, t) J_n(kr) e^{in(\phi_q + \delta\phi)}. \tag{8}$$

Comparing (4) and (8), the soundfield coefficients of the reproduced soundfield becomes

$$\beta_n(\omega, t) = \beta_n^d(\omega, t) e^{-in\delta\phi}. \tag{9}$$

In this scenario the perturbation factor $e^{-in\delta\phi}$ is a bounded function that gives rise to a special result. From (5) and (9), the reproduced soundfield coefficients become

$$\beta_n(\omega, t) = \begin{cases} (-i)^n e^{-in(\phi_y + \delta\phi)} & : \text{Plane wave}, \\ \mathscr{H}_n^{(2)}(ky) e^{-in(\phi_y + \delta\phi)} & : \text{Point source}. \end{cases} \tag{10}$$

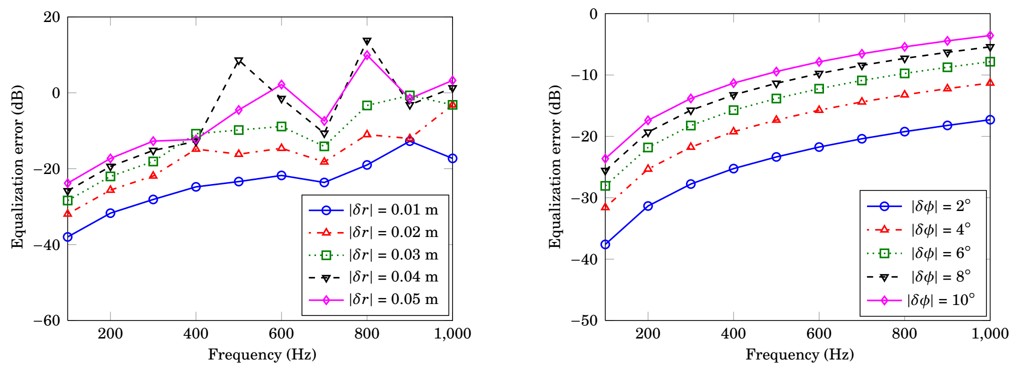

(a) Radial perturbation

(b) Angular perturbation

FIGURE 2: Normalized equalization error for plane wave and point source reproduction.

Equation (10) suggests that angular perturbations in the equalizer microphone locations will simply result in a rotation of the desired soundfield, the impact of which may be negligible on the quality of the reproduced soundfield.

RESULTS AND DISCUSSION

We evaluate the equalization and reproduction performance through simulations of a 2-D reverberant room for perturbations in the equalizer microphone positions. We consider a room with the dimensions 5 m × 6.4 m and a wall absorption coefficient of 0.36, where the region of interest $\mathscr{R}$ is a 0.3 m radius ($\approx 1.12\lambda$ at 1000 Hz) area centred at (2.4 m, 3.8 m) and reverberation is simulated using the image source method in [13]. The soundfield reproduction system is designed for frequencies up to 1000 Hz, and utilises 19 equalizer microphones positioned at the edge of $\mathscr{R}$ and a 2 m radius concentric circular array of 24 loudspeakers.

The robustness of the equalization process is evaluated at the radial perturbations $|\delta r| = \{0.01\text{ m}, 0.02\text{ m}, 0.03\text{ m}, 0.04\text{ m}, 0.05\text{ m}\}$ and angular perturbations $|\delta\phi| = \{2°, 4°, 6°, 8°, 10°\}$. The chosen perturbations correspond to similar mispositioning of the equalizer microphones, and can be used to compare the performance implications of the two types of perturbations. The performance measures used to evaluate the room equalizer are as follows.

1. Normalized Equalization Error:

$$\mathscr{E}(\omega,t) = 10\log_{10}\frac{\left|\left[\boldsymbol{\beta_n}(\omega,t)-\boldsymbol{\beta_n^d}(\omega,t)\right]^H\left[\boldsymbol{\beta_n}(\omega,t)-\boldsymbol{\beta_n^d}(\omega,t)\right]\right|}{\left|\boldsymbol{\beta_n^d}(\omega,t)^H\boldsymbol{\beta_n^d}(\omega,t)\right|}, \tag{11}$$

where

$$\boldsymbol{\beta_n}(\omega,t) = \left[\begin{array}{ccc}\beta_{-N}(\omega,t) & \cdots & \beta_0(\omega,t) \quad \cdots\beta_N(\omega,t)\end{array}\right]^T,$$

$$\boldsymbol{\beta_n^d}(\omega,t) = \left[\begin{array}{ccc}\beta^d_{-N}(\omega,t) & \cdots & \beta^d_0(\omega,t) \quad \cdots\beta^d_N(\omega,t)\end{array}\right]^T.$$

2. Normalized Region Reproduction Error:

$$\mathscr{T}(\omega,t) = 10\log_{10}\frac{\int_{\mathscr{R}}\left|Y(\mathbf{x};\omega,t)-Y^d(\mathbf{x};\omega,t)\right|^2 \mathrm{d}a(\mathbf{x})}{\int_{\mathscr{R}}\left|Y^d(\mathbf{x};\omega,t)\right|^2 \mathrm{d}a(\mathbf{x})}, \tag{12}$$

where $\mathrm{d}a(\mathbf{x}) = x\,dx\,d\phi_x$ is the differential area element of $\mathbf{x}$, and $Y(\mathbf{x};\omega,t)$, $Y^d(\mathbf{x};\omega,t)$ are the reproduced and desired soundfield pressure at $\mathbf{x}$ respectively.

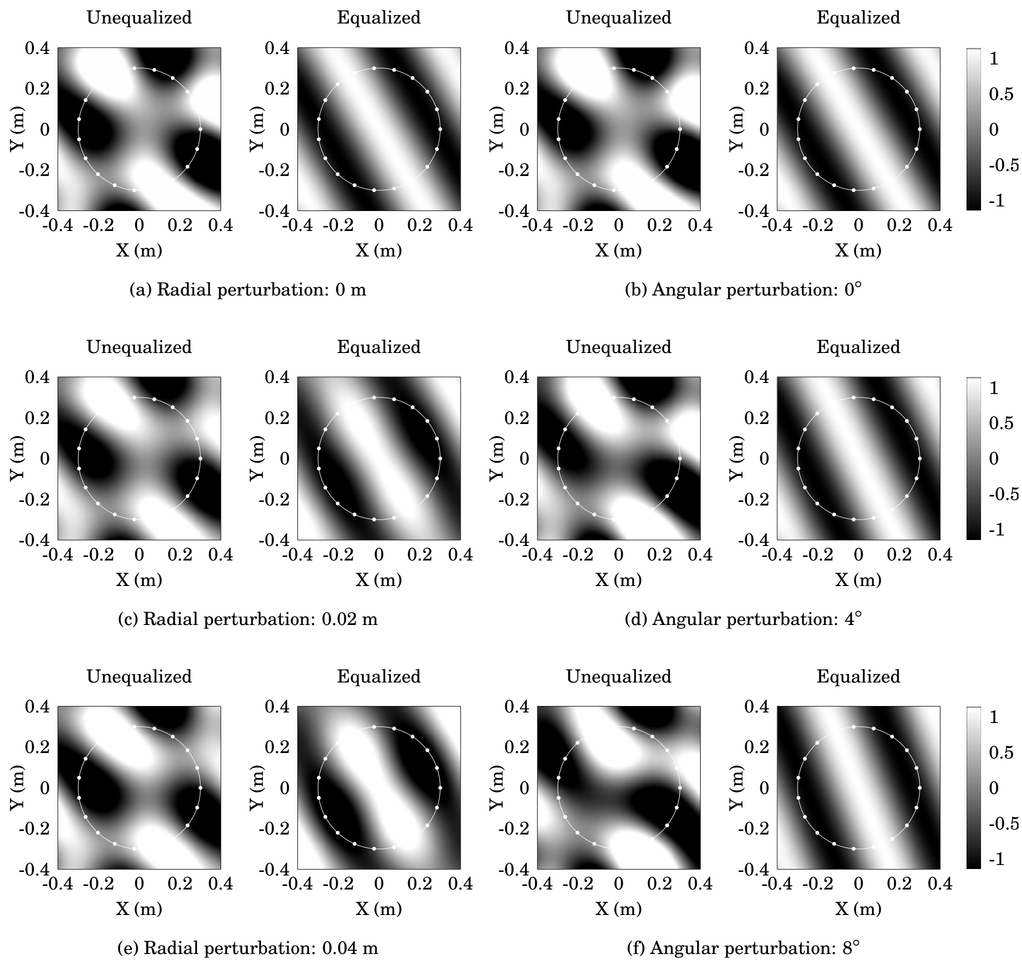

(a) Radial perturbation: 0 m

(b) Angular perturbation: 0°

(c) Radial perturbation: 0.02 m

(d) Angular perturbation: 4°

(e) Radial perturbation: 0.04 m

(f) Angular perturbation: 8°

FIGURE 3: Reproduction performance of a 700 Hz plane wave incident from $\phi_y = \pi/3$. The white dotted circle indicates the region of interest and equalizer microphone locations.

Equalization Performance

Figure 2 illustrates the normalized equalization error for different perturbations of the microphone locations, which behaves similarly for both plane wave and point source reproduction. As expected from (7), the normalized equalization error for radial perturbations is unbounded, and varies with the operating frequency and the level of perturbation. This is clearly seen as peaks in the equalization error at the higher frequencies and perturbations, where zeros of the Bessel functions are more likely to be encountered. The equalization error behaviour at smaller radial perturbations is similar to that of the diffuse-field reverberation model used in [5], and suggests that the effects of radial perturbations can be minimized by limiting $|\delta r|$ with respect to k.

The normalized equalization error for the angular perturbations follow the bounded behaviour suggested in (9), where the error increases with frequency due to the accumulated error of a larger number of active modes at higher frequencies. The equalization error at smaller perturbations demonstrates a similar behaviour as the smaller radial perturbations, but is limited to values below 0 dB for the simulated conditions. This suggests that the equalization error due to angular perturbations of the equalizer microphone locations are less significant, and implies that the room equalizer is more robust to angular perturbations of microphone positions.

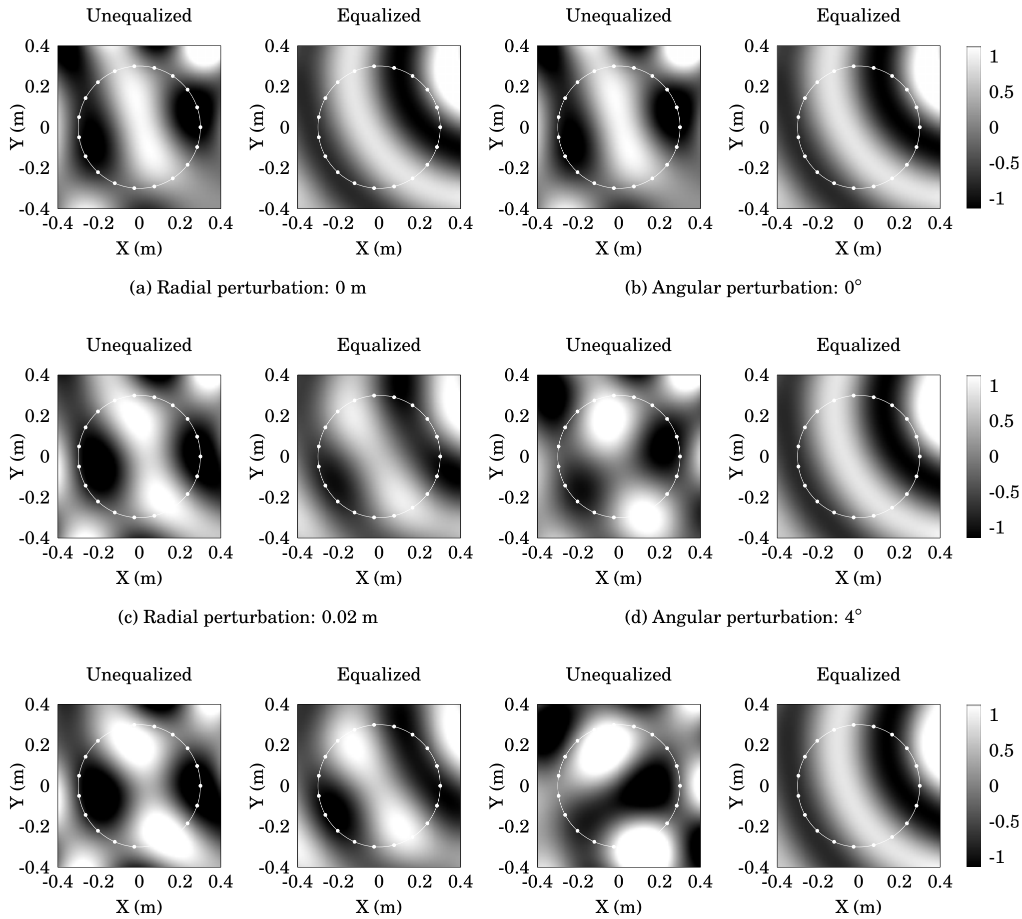

(a) Radial perturbation: 0 m (b) Angular perturbation: 0°

(c) Radial perturbation: 0.02 m (d) Angular perturbation: 4°

(e) Radial perturbation: 0.04 m (f) Angular perturbation: 8°

FIGURE 4: Reproduction performance of a 700 Hz point source at $\mathbf{y} \equiv (0.6 \text{ m}, \pi/3)$. The white dotted circle indicates the region of interest and equalizer microphone locations.

Region Reproduction Performance

Figures 3 and 4 illustrate the unequalized and equalized reproduction performance for a plane wave and point source at 700 Hz. Subfigures (a) and (b) indicate that good reproduction performance can be achieved in the region $\mathscr{R}$ when the microphone locations are not perturbed. However, the effects of radial perturbations become significant with larger perturbations, as with the equalization behaviour described in the previous subsection. In the case of angular perturbations, a rotation of the reproduced soundfield is observed. This becomes clear when subfigures (b), (d) and (e) are compared, which indicates that the reproduced soundfield rotates by some $\delta\phi$ corresponding to the angular perturbation. Comparing Figures 3 and 4, it is seen that the reproduction of the plane wave is more robust to radial variations of the microphone positions.

The normalized region reproduction error calculated in the region of interest $\mathscr{R}$ is illustrated in Figures 5 and 6. The region reproduction error behaves similar to the equalization error in Figure 2, where radial perturbations lead to significant errors. The peaks in the error function due to radial perturbations can be attributed to the zeros in the denominator Bessel function in (7), and is similar to the equalization error behaviour in Figure 2. The normalized region reproduction error ranges between -40 dB to 40 dB in the operating frequency range for the reproduction of both the plane wave and point sources. Normalized region reproduction error

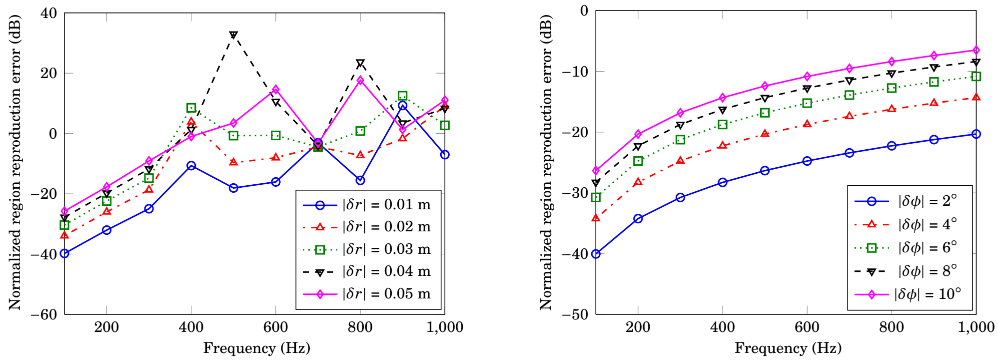

(a) Radial perturbation

(b) Angular perturbation

FIGURE 5: Normalized region reproduction error for plane wave reproduction.

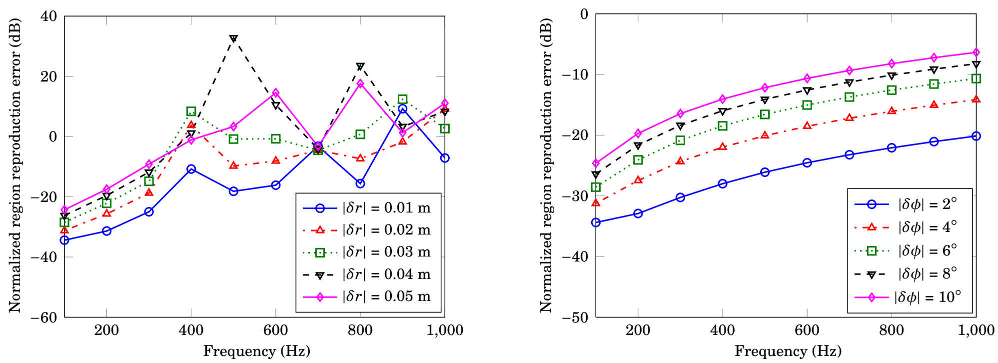

(a) Radial perturbation

(b) Angular perturbation

FIGURE 6: Normalized region reproduction error for point source reproduction.

due to angular perturbations are between -40 dB and -5 dB and is below the acceptable error threshold of -10 dB for angular perturbations less than $\lambda/10$ (where λ is the wave length).

The following conclusions can be drawn from these results. Firstly, robust equalization of large areas ($r > \lambda/10$) is possible using a number of carefully positioned equalizer microphones at the edge of the equalization region, even though the microphone positions are perturbed. Secondly, the maximum allowable perturbations to the microphone location are still limited to $\lambda/10$ as shown in [5]. Finally, the effect of radial perturbations play a significant role in the equalization process and is the dominant factor that results in higher reproduction error at larger perturbations.

CONCLUSION

In this work, we have evaluated the robustness of the region equalization process to positioning errors of the equalizer microphones in a soundfield reproduction application. We show that mispositioning of the equalizer microphones can be characterised in terms of radial and angular perturbations. Next, we show how radial perturbations results in an unbounded normalized region reproduction error, while angular perturbations simply result in a rotation of the desired soundfield. Simulations results suggest that radial perturbations dominate the region reproduction error performance, and is exacerbated at particular frequencies and perturbations. It is also seen that the region equalization process is more robust in the presence of angular perturbations of the equalizer microphone positions; a property that may prove useful in practical applications.

REFERENCES

[1] S. J. Elliott and P. A. Nelson, "Multiple-point equalization in a room using adaptive digital filters", J. Audio Eng. Soc. **37**, 899–907 (1989).

[2] T. Betlehem and T. D. Abhayapala, "Theory and design of sound field reproduction in reverberant rooms", J. Acoust. Soc. Am. **117**, 2100–2111 (2005).

[3] S. Spors, H. Buchner, R. Rabenstein, and W. Herbordt, "Active listening room compensation for massive multichannel sound reproduction systems using wave-domain adaptive filtering", J. Acoust. Soc. Am. **122**, 354–369 (2007).

[4] M. R. Schroeder, "Statistical parameters of the frequency response curves of large rooms", J. Audio Eng. Soc. **35**, 299–306 (1987).

[5] B. D. Radlovic, R. C. Williamson, and R. A. Kennedy, "Equalization in an acoustic reverberant environment: robustness results", IEEE Trans. Speech and Audio Process. **8**, 311–319 (2000).

[6] J. Mourjopoulos, "On the variation and invertibility of room impulse response functions", J. Sound Vib. **102**, 217–228 (1985).

[7] D. B. Ward and T. D. Abhayapala, "Reproduction of a plane-wave sound field using an array of loudspeakers", IEEE Trans. Speech and Audio Process. **9**, 697 –707 (2001).

[8] M. A. Gerzon, "Periphony: With-height sound reproduction", J. Audio Eng. Soc. **21**, 2–10 (1973).

[9] M. A. Poletti, "Three-dimensional surround sound systems based on spherical harmonics", J. Audio Eng. Soc **53**, 1004–1025 (2005).

[10] A. J. Berkhout, "A holographic approach to acoustic control", J. Audio Eng. Soc **36**, 977–995 (1988).

[11] A. J. Berkhout, D. de Vries, and P. Vogel, "Acoustic control by wave field synthesis", J. Acoust. Soc. Am. **93**, 2764–2778 (1993).

[12] E. G. Williams, *Fourier Acoustics: Sound Radiation and Nearfield Acoustical Holography* (Academic Press) (1999).

[13] J. B. Allen and D. A. Berkley, "Image method for efficiently simulating small-room acoustics", J. Acoust. Soc. Am. **65**, 943–950 (1979).